J. Condensed Matter Nucl. Sci. 29 (2019) 75–84

Research Article

Cavitation Effects on Various Metals in D_2O

Thomas N. Claytor*
High Mesa Technology, Los Alamos, NM, USA

Roger S. Stringham†
Firstgate Energy, Kauai, Hi, USA

Malcolm M. Fowler‡
McFarland Instrumentation Services Inc., ESPANOLA, NM 87532- 3502, USA

Abstract

Cavitation at high frequency in close proximity to metal surfaces was investigated in D_2O. A new miniaturized cavitation system was operated at 1.7 MHz and was small enough to fit into a sensitive Seebeck calorimeter. The 1.7 MHz reactor was designed to hold 20 g of D_2O or H_2O. The cells were operated in a pulsed mode for 1 or 2 min and then allowed to cool in the calorimeter. Target foils were placed in close proximity to the transducer and different foils show a maximum of about 13% change in measured excess heat output. Tritium measurements were made on the resulting liquid and showed a small initial increase. However, longer runs did not show a linear increase in tritium as the cavitation times were increased. No detectable signals were measured on a pancake gamma detector placed below the cavitation cells. Many different target foils (TF) ($7 \times 19 \times 0.1$ mm) were run in the system. A few showed some interesting surface features.
 ISSN 2227-3123

Keywords: Bubble collapse, Cavitation, Cavitation damage, LENR, Particulate generation, Ultrasound

1. Introduction

Many have speculated that cavitation with either single or multiple bubble could result in dd fusion in the presence of D_2O or other deuterided liquids [1–3]. Here, we investigate cavitation not only in the liquid but primarily as it impinges on different metal surfaces. Cavitation damage on metals in H_2O is well known [4]. Less studied is cavitation damage in metals immersed in D_2O [5–10]. In particular, we investigated the assertion by Stringham [6–10] that very anomalous effects occur when metal foils are immersed in a cavitation field at fairly high frequencies.

*Corresponding author. E-mail: Claytor@att.net.
†E-mail: Rogerssbiz@gmail.com.
‡E-mail: Malcolm-fowler@zianet.com.

 ISSN 2227-3123

Cavitation damage is typically seen at low frequencies (30 kHz) where the bubble can grow to microscopic dimensions (>100 μm) and with about 90 nJ energy. At the high frequencies ($\sim$1.7 MHz) of this study the energy contained in a single bubble is small, but there may be millions of bubbles. Little work has been done to characterize the damage or the damage products from the metal surface-cavitation interaction at these frequencies because such low energies are not expected to produce much surface damage [4]. The cavitation threshold in an ideal fluid is thought to be very high (>800 W/cm^2) at the frequency used in this study. However, our liquid is less than ideal because the target metal and transducer will shed oxide particles and, in addition, there may be nano-cavities [4] in the liquid formed during the cavitation. Thus, the cavitation threshold is lowered substantially ($\sim$20 W/cm^2). This particular experiment has many parameters that are difficult to control and will impact the reproducibility of the experiments. With further refinements, we expect the reproducibility to improve. The basic purpose of this research is to determine if the "Stringham effect" can be reproduced and in what metals is it most evident. By the term "Stringham Effect" we are referring to anomalous behavior of cavitation impinging on a metal. This could be the appearance of excess heat, helium or tritium in the liquid or metal, or other elements that were not initially present in the liquid or metal.

2. Procedure

Tritium was measured with a Beckman LS6500. A unique feature of the scintillation counter is that it is totally enclosed in a sealed volume to reduce radon prodigy infiltration and has a real time radon monitor in the enclosure. This allows for a very consistent and low background. Ultima Gold (Perkin Elmer scintillation fluid) was used for all measurements in low background poly vials. Vials were typically counted four times, no less than a day apart, to ensure no short half lived isotopes were present.

Radiation detection directly from the cavitation cell or foil (post run) was done with an RM-80 pancake detector (Aware Electronics) and Silicon Surface Barrier Detectors from ORTEC and an AMPTEK 8000A multichannel analyzer.

Excess heat measurements were made in a custom calorimeter that was obtained from Coolescence (Fig. 1). The calorimeter outer chamber is temperature controlled to 0.1°C (via a heat exchanger and water chiller) and the interior envelope is 86.3 $\times$ 38.1 $\times$ 29.2 cm (l,w,h). Located in the controlled environment is the inner calorimeter chamber that has an interior volume of 18.0 $\times$ 11.5 $\times$ 13.0 cm (l,w,h). The entire top of the inner chamber consists of a Peltier sensing element. Typically, the outer chamber was held at 19–20°C and, at this temperature, the sensitivity of the calorimeter was 27.1 mV/W at a 22 W input.

SEM measurements were made with a Tescan Vega with a Bruker EDX. ICPMS analysis was done by A&B Labs. Houston TX. using an Agilent 7700 and 7900.

3. Cavitation Cells

Several iterations of the cavitation cells were investigated for this study. Initially an all acrylic cell was used, but it was found that the heat from the transducer and the heat from the absorbed ultrasonic beam would eventually distort the acrylic body resulting in leaks. Acrylic bodies were used exclusively for long runs to collect nanoparticles for analysis in the ICPMS. The final design of the cells for use in the calorimeter was made with an aluminum transducer holder and a glass tube with an acrylic top and O-ring seal. This is shown in Fig. 2. To minimize pressure buildup in the cell, the units were only run for a maximum of 2 min. The transducers were 1.7 MHz PZT disks 20 mm diameter by 1.3 mm thick and were glued into the aluminum holder with thermosetting glue. The transducers were from various sources (but all PZT) having different working surfaces. In some cases the surface electrode was silver, or stainless steel or even Ni with a TiN coating. Since all the transducers had different efficiencies and even different units of the same model varied by 20%, it was important that during the calorimeter tests of different foils the same transducer

Figure 1. Coolescence calorimeter, outer box (*left*), and inner chamber with Peltier elements (*right*).

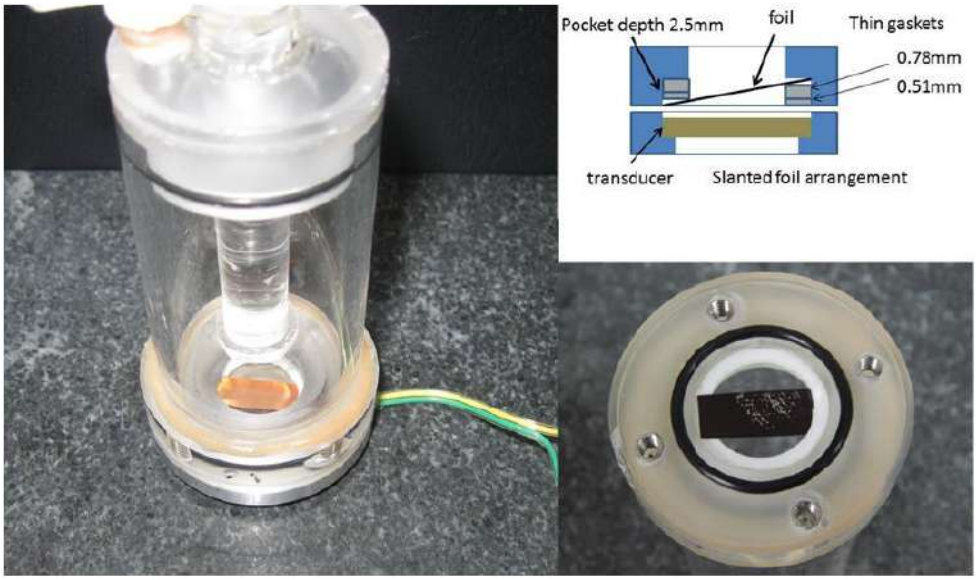

Figure 2. Cavitation cell with reflector and copper sample (*left*), arrangement of foil in cell and a Ni foil that was painted to show cavitation streaks and pits after a short run (*right*).

was used. For electrical input powers of greater than 30 W the transducers would eventually fail (due to the electrical contacts or surface foil delamination). Thus, for all the data reported here for calorimetric measurements, the power input to the transducer was kept to about 18–24 W.

4. Materials

The foils (technical grade) used in this study were 19 mm in length and 7 mm wide by 250 μm or 125 μm thick. The D_2O was from Cambridge Isotopes (99.9%) and the H_2O was distilled water. The Cambridge Isotopes D_2O contained 90 or 7 dpm per ml of tritium depending on the batch. The water did not contain any detectable tritium (<1.5 dpm). Prior to the experiments, the D_2O or H_2O was degassed in a vacuum chamber for a few minutes. After the vacuum process, Argon was introduced into the chamber. Most runs were performed with an Argon cover gas.

5. Experimental

Initially it was uncertain if strong cavitation could be generated at the high frequencies used in this study because of the low energy contained in the bubble. To determine that indeed there was cavitation, several foils were painted with a thin layer of black paint. After exposure in the cell, these foils would often show small round <30 μm features where the paint had been removed and the specular reflection from the metal surface sometimes showed a frosted texture. However, the density of these features varied considerably from run to run, sometimes none were seen and other times there was a high density. This was attributed to the fact that in the near field of the transducer the intensity varies rapidly with distance from the transducer surface and also with the liquid temperature. Since these parameters could vary from run to run, it was decided to slant the foil slightly to present at least some of the foil surface at an intensity maxima. The microscopic pits could be in lines or in a circular pattern depending on the standing wave pattern in the liquid or on the foil.

Cavitation was also detected using a thin (0.02 mm) piezoelectric transducer attached to the side of the cell. When the system was run at 1.7 MHz, there was a broad peak in sound intensity (as measured by the probe transducer) centered near 200 kHz suggesting the maximum bubble size was 10 μm. It was found that in clean, cold, degassed D_2O or H_2O the intensity of the 200 kHz spectra dropped 10 dB within the first 20 s of operation, indicating that perhaps the bubbles became gassy or the particulates were nucleating the cavitation.

It should be noted that a thermocouple on the backside (side not in contact with the liquid) of the piezo driver would often rise to temperatures >100°C within 10 s after the power was applied. Because the temperature is constantly changing during a run, it was difficult to maintain the resonant condition for very long, if just a driver amplifier was used at a constant frequency. So, for this study we used a custom oscillator that maintained the resonant condition for the transducer as the temperature of the piezoelectric transducer and water increased. Our goal was to hold the power constant to the transducer to within 5–10% during a 1 or 2 min run. For each material used, the power delivered to the transducer would be slightly different. Therefore, the drive was adjusted to maintain about 22 W to the transducer. The reason for this was to present to the calorimeter and the electronic power measurement circuit the same power for each foil. Our objective was to determine if there is a difference in heat output between metals under the influence of the cavitation. The weight of the cell was measured prior to the run and after to determine if any water or D_2O had been lost. If the seal obviously leaked or more than 10 mg of water was lost, the run was discarded.

6. Power Measurements

To measure the RF power to the transducer a Tektronix CT-2 current transformer was used for the current measurement, and a Tektronix 2220 voltage probe measured the voltage across the transducer leads. Because the current transformer

is nominally accurate to within 2% and the voltage probe is accurate to within 2% it is not expected that our AC measurement compared to a DC measurement of a purely resistive load would give agreement better than 5%. Thus, we restrict ourselves to presenting comparative outputs from each different foil. A Tektronix TDS 2024B scope (200 MHz, 2 Gs/s) was used to make the measurement of $V \times I$ for each point on the voltage and current waveforms. Then the resultant waveform was summed over an integral number of cycles to obtain the power measurement. All measurements were made without changing any of the gain ranges on the scope between runs with different foils. It was found that any gain changes on the scope introduced an unacceptable change in apparent power. PC data analysis and acquisition software (Keysight VEE) was optimized to acquire a power reading every 250 ms resulting in 240 power samples for a 1 min run. The Seebeck calorimeter output (voltage) was recorded every 2 s along with room, interior box and Peltier fin temperature using K-type thermocouples. These measurements were made with a Keithley 2700 multichannel scanner connected to a PC.

7. Results

Shown in Fig. 3 are SEM images of a PdAg 2% foil after several 2 min runs in D_2O at 30 W (1.7 MHz) input power to the transducer. The left image shows a large (>100 μm) feature that was formed in the center of the plate. The material was found to contain oxides of Na, K, Al, Ca, Mg, Si, and Cl, S and P by EDX. After the material was removed a rather large hole in the surface was revealed. EDX focused on the interior of the large hole and small hole clusters showed the same EDX signature as the large feature.

Figure 4 is an SEM image of an Ag foil that had been run under similar conditions to the PdAg 2% foil. It can be seen that a large consolidated clump of material is in the center of the foil where the acoustic intensity is expected to be highest. It should be noted that under the large clump in the right image a hole was found suggesting that the material on the surface originated from the hole. Since no SEM images were made of the foils prior to the sonic irradiation it

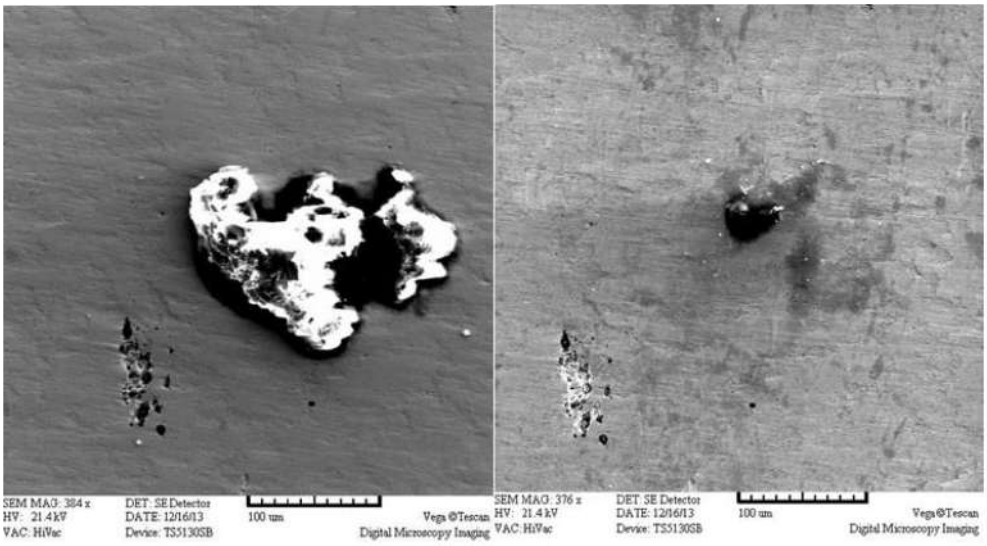

Figure 3. Material found on a PdAg 2% foil after runs at 1.7 MHz. Small holes are to the lower left of the large feature (*left*). After the large feature was removed a large hole was revealed (*right*).

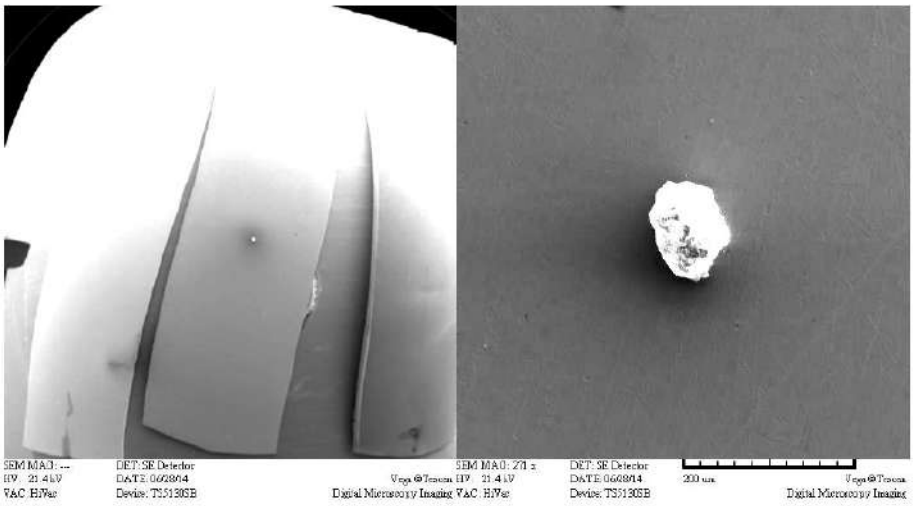

Figure 4. Ag foil (left low mag, right high mag) showing clump of material similar to that found on the PdAg 2% foil. When the material on the surface was removed a hole similar to the one found on the PdAg 2% foil was revealed.

cannot be ruled out that the holes were not initially present. However, each foil was initially visually inspected under $\times 10$ magnification and the holes were not noticed.

Shown in Fig. 5 is a picture is of a pure Ni plate that had a stripe of round Ni particles deposited on the surface facing the transducer. These were not present prior to the cavitation run as determined by visual inspection. None of

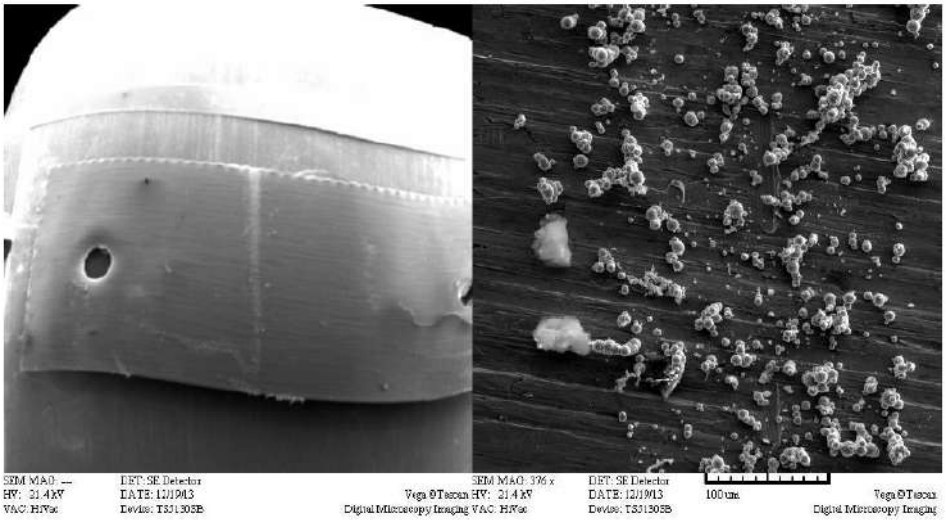

Figure 5. Ni foil 7 mm wide showing stripe of Ni particles (*left*), close up of Ni balls in stripe (*right*).

Table 1. Results of ICPMS (elements not listed in the table were below detection limits).

Run	Ni, D_2O 7.6 h	PdCu, D_2O 3.5 h	PdRhCoB, D_2O 9.3 h	PdB, D_2O 10.5 h	PdAg, D_2O 11.75 h	Cambridge isotopes D_2O unused material	Detection limit mg/l
Al mg/l	0.0071	0.0057	0.024	0.0068		0.0048	0.002
Sb	0.012	0.012	0.023	0.014	0.010	0.012	0.0012
Cr	0.0016			0.0014			0.0012
Cu	0.0042	0.0076	0.0037	0.0066	0.011	0.0014	0.0012
Pb	0.0048	0.002		0.0031			0.0012
Ni	0.0036					0.0014	0.0012
Ag		0.003		0.0086	0.0083		00012
Na	3.3	1.12	4.05	3.8	4.27	2.4	0.25
Zn	0.0092	0.015	0.018	0.0088	0.025		0.005

the foils showed any radiation over background when placed on the pancake Geiger detector (RM-80). However, this measurement was not done until several hours after the runs.

Given the apparent fact that certain elements not initially present in the foil were ejected from the foil, we ran several foils for an extended time ($\sim$10 h) (but at lower power levels of 20 W) to attempt to build up particulates in the D_2O. Light scattering (405 nm) revealed that in PdB, PdCu, PdAg 2% and Ni foils nano-particulates were present. In addition, some of the particulates strongly fluoresced in the infrared. ICPMS was performed on 10–20 g of the D_2O from these runs as well as a blank D_2O sample. Because the samples were relatively small, the ICPMS analysis was not as sensitive as desired, in particular Na, K, Mg, Ca, Fe were only able to be detected at the 250 μg/l level, the other 20 elements (Al, Sb, As, Ba, Be, Cd, Cr, Co, Cu, Pb, Mn, Mo, Ni, Se, Ag, Tl, Th, Ti, V, and Zn) were detectable at the 5–1 μg/l level. The results of heavy water analysis are shown in Table 1.

The pure CI D_2O is seen to have Al, Sb, and Na at values well over the detection limit, the other elements in the D_2O, Cu and Ni are at the detection limit for the instrument. Zn is found in all the post processing samples, but ZnO is a ubiquitous material often found in ceiling tiles. Interestingly only a modest amount (2.5$\times$ background) of Ni was found in the Ni sample. One might expect to find Pd in the analysis, but this was not detected, due to the fact that its detection required a more complicated digestion. Co was also not detected in the PdRhCoB sample. This along with the paucity of Ni in the Ni sample leads one to believe that the cavitation erosion of the parent metal was not a vigorous as one might have expected.

The highest sodium level is obtained from the sample that was run the longest and Cu is also present at the highest concentration in the sample that was longest run. Interestingly, the face of the transducer in these runs was stainless steel (Fe 66.4%, Cr 16.6%, Ni 13.7%, Mo 1.5%, Mn 1.28%, and Cu 0.41%). Thus, one would expect to see elevated amounts of Fe, Cr, and Ni in each sample. The data is suggestive that some of the material seen in the eruptions (in Figs. 3 and 4) has been detected as nano-particulates in the liquid especially after longer runs. Given the fact that others have found similar elements in their systems, more work should be done to confirm these results [12].

Not all of the material generated in these cavitation runs ends up in the liquid. Some is deposited on the transducer and foil. Very small amounts of material can be detected in the SEM and analyzed by the EDX if it occurs as particles on the foil surface. For instance, the PdB sample had Cu, Pt, and Pd particulates present on the foil, the PdRhCoB had a cluster of Fe, Mn, and Co particulates. Similarly, a Pure Pd sample showed a cluster of Si, Ni, Cu, Zr, S, Al, Mn, and Fe as well as Pd particulates. Because of the micro-nature of the particulates (usually <5 μm) and the fact that they are sparse, they would not be detectable by ICPMS even if dissolved in the liquid. Even the large objects on the surfaces in Figs. 3 and 4 would not have been detected in the ICPMS analysis, even if the material was completely dissolved because of the number of elements present.

8. Calorimetry

The Coolescence calorimeter was slightly modified to make it more efficient. Aluminum foil (250 μm thick) was added to all the walls of the calorimeter, except the upper surface where the Peltier elements were located. The aluminum plate that held the Peltier elements was painted black on the interior to more effectively absorb the heat. A fixture in the calorimeter held the cavitation cell in the same location for each run and because the transducer gets hot, during a run, a fan was placed in the fixture that blew directly on the transducer. Since the transducers could not be run for more than 2 min at a time without severe heating, pulsed calorimetry was used for the tests. In the pulsed mode, RF was applied for 1 or 2 min, the calorimeter responded promptly and then the response decayed over a period of 2–3 h.

To compare each metal against the others in D_2O and with the no-sample runs in H_2O and D_2O, the peak response and total integrated heat was measured during a 3 h period and subtracted from the baseline. Repeated measurements using a resistor as a calibration show that the repeatability was $\pm 1.7\%$ for the 1 min runs and $\pm 0.5\%$ for the 2 min runs. The largest non-random error in the calorimeter output is due to the temperature control in the lab room (and thus the outer calorimeter chamber) that can vary depending on the state of the AC or heating system. The peak value of the heat output was less sensitive to the ambient changes since that measurement could be completed in 10 min rather than 3 h. About 100 calorimeter runs were made to assess apparent heat from various foils and background runs.

Figure 6 summarizes the peak heat data obtained for various foils and no foil. The conditions for the calorimeter runs were that the sample and inner chamber of the calorimeter was 20°C and the power applied (21–24 W) to the transducer was on for 60 s and normalized to 22 W. Twenty grams of low tritium D_2O was used for all runs. Several runs on the same sample were performed and the results in Fig. 6 are the average of those runs. The difference between the heat from the highest sample and the no sample run was 13.8% with a maximum error of 3.4%, thus the data has a significance of about 4σ.

Interesting, among the top four alloys are PdB and PdRhCoB alloys that are implicated in electrochemical excess heat experiments [13] and tritium production experiments [14]. Excess heat from Cu and Nb foils is unexpected since there is no prior indication that these materials would be active in excess heat experiments. But given the large uncertainty in the experiment, these data should be revisited. Improvements to the calorimeter are being made and further work will utilize 2 min runs and more stable temperature regulation of the outside box.

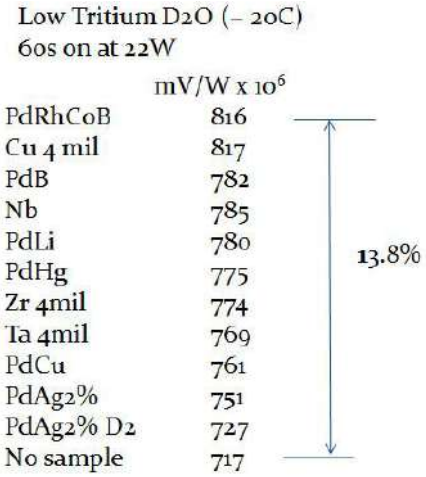

Figure 6. Ranking of foils.

The excess power measured here is a small fraction of the total power supplied to the system. For instance, for 22 W delivered to the transducer, 32 W has to be input to the resonator board. The maximum excess power is about 2.8 W for the data in Fig. 6. However, this is consistent with the excess power often reported by Stringham for operation at this frequency.

9. Tritium Results

Active material often results in the appearance of tritium in the D_2O. In many instances the tritium will increase initially, then either level off or decrease slightly. Here we adopted multiple foil experiments to determine if any one of many foils produced excess tritium. In other words, the same low tritium D_2O was used for each successive foil. The resulting low tritium D_2O was filtered (0.1 μm filter) or distilled prior to scintillation counting. Neither process removed all the nano-particulates. After running multiple samples for 76 min (1 min on and 5–10 min off to cool down), the excess tritium generation rate confidence was 2σ (79.5 pCi/h $\pm$ 42) over the background. This rate is significantly higher than most of the rates obtained from gas discharge systems [14]. However, the uncertainty is larger than in those experiments. PdRhCoB and PdCu were run independently (for >3 h) and gave low rates of tritium generation (5.5 pCi/h and 10 pCi/h) that also did not exceed the 2σ confidence level. The fact that longer runs yielded more tritium is encouraging, however, the longer the run, the lower the rate.

10. Conclusion

The data presented here indicates that cavitation on metals in D_2O and perhaps H_2O can produce anomalous results that are defined as the "Stringham effect" after Roger Stringham, who originally investigated these phenomena. This includes the evidence for the appearance of elements not originally present or elements in unusual forms in the system after cavitation. While these supposed transmutation effects occur also in electrochemical cells, the electrochemical cells contain a soup of chemicals that often are claimed to be the source of the impurities. In the present study, the materials are clean foils and pure D_2O or H_2O with no additives other than perhaps an Argon cover gas.

Tritium in small but consistent amounts has been found in the liquid after D_2O runs. No mixed D_2O/H_2O runs have been done, in this study, but they would be the next step since a D_2O/H_2O ratio of 20% seemed to be more effective than pure D_2O in producing tritium in catalytic systems based on our prior unpublished work.

The lack of X-rays or gammas is the most obvious problem when trying to explain that this process is nuclear. However, if the energy is less than 10 keV then it is doubtful that the X-rays would escape from the cells. Some foils did pick up radon prodigy (as determined by the SSD detector) after removal from the cell, but those can be easily discriminated from longer term emissions from the foils. Nevertheless, the preponderance of data presented here definitely supports Stringham's claims of anomalous behavior in these systems.

Acknowledgements

We would like to acknowledge the generous support of Dewey Weaver and J.T. Vaughn of Industrial Heat LLC, and Rick Cantwell and Matt McConnell of Coolescence LLC. Edmund Storms provided very useful discussions/suggestions and access to his SEM and EDX for this work.

References

[1] W.C. Moss, D.B. Clarke, J.W. White and D.A. Young, Sonoluminescence and the prospects for table-top micro-thermonuclear fusion, *Phys. Lett.* A **211** (1996) 69.

[2] R.P. Taleyarkhan et al., Evidence for nuclear emissions during acoustic cavitation, *Science* **295** (2002) 1868.

[3] Nanospire Inc.
[4] D.G. Shchukin, E. Skorb, V. Belova and H. Mohwld, Ultrasonic cavitation at solid surfaces, *Adv. Materials* **23**(17) (2011) 1922–1934.
[5] J. Jorne, Ultrasonic irradiation of deuterium-loaded palladium particles suspended in heavy water, *Fusion Technol.* **29** (1996) 83.
[6] R.S. Stringham, When bubble cavitation becomes sonofusion, in *237rd ACS National Meeting*, Salt Lake City, 2009. http://citeseerx.ist.psu.edu/viewdoc/download?doi=10.1.1.380.6715&rep=rep1&type=pdf.
[7] R.S. Stringham, When bubble cavitation becomes sonofusion, *J. Condensed Matter Nucl. Sci.* **6** (2012) 1–12.
[8] R.S. Stringham, Sonofusion produces tritium that decays to helium three, *ICCF 15*, V. Violante and F. Sarto (Eds.), Oct. 5–9, 2009, p. 57
[9] R.S. Stringham, Deuteron plasmas driven to neutrality and ^{4}He, *ICCF 21*, S. Katinsky and D. Nagle (Eds.), University of Colorado State, Fort Collins CO, June 3–8, 2018, to be published in *J. Condensed Matter Nucl. Sci.*
[10] R. Stringham, Helium measurements from target foils at LANL and PNNL, *J. Condensed Matter Nucl. Sci.* **24** (2017) 284–295.
[11] M. Alheshibri, J. Qian, M. Jéhannin, and V.S. J. Craig, A history of nanobubbles, *Langmuir* **32** (2016) 11086–11100.
[12] Arik El-Boher, University of Missouri, private communication.
[13] M. Miles, K.B. Johnson and M.A. Imam, Electrochemical loading of hydrogen and deuterium into palladium and palladium–boron alloys, in *Sixth Int. Conf. on Cold Fusion*, *Progress in New Hydrogen Energy*, 1996, p. 208.
[14] T.N. Claytor et al., Tritium evolution from various alloys, *LAUR* 98-2697.